Toroidal plasmas

Overview

1. Equilibrium

(a) Context (Alfvén wave dynamics, statement of the equilibrium problem)

(b) Cylindrical equilibrium (rotational transform)

(c) Toroidal equilibrium (Grad–Shafranov equation, scaling)

(d) Mapping for stability (straight field line coordinates)

2. Waves and instabiities

(a) Toroidal wave equation

(b) Field line resonances and ballooning modes

(c) Numerical stability (ideal and resistive)

(d) MHD spectroscopy of tokamaks

Context: plasma dynamics

time scale	tokamak	corona	
very fast	$10^{-9}\,\mathrm{s}$	$10^{-6}\,\mathrm{s}$	$\Rightarrow$ *Kinetic waves & instab.*
fast	$10^{-6}\,\mathrm{s}$	$10\,\mathrm{s}$	$\Rightarrow$ *MHD waves & instab.*
slow	$10^{-3}\,\mathrm{s}$	$10^{4}\,\mathrm{s}$	$\Rightarrow$ *Equilibrium*
very slow	$1\,\mathrm{s}$	$10^{11}\,\mathrm{s}$	$\Rightarrow$ *Transport*

$\Rightarrow$ **MHD range is the most robust part**

- *MHD equilibrium & stability* absolute requirements for fusion in tokamaks.
- *MHD spectroscopy:* diagnostics of laboratory as well as astrophysical plasmas.

Alfvén wave dynamics

- *Alfvén waves are point perturbations propagating along the magnetic field lines* (Friedrich's diagram).

  $\Rightarrow$ *Alfvén waves 'sample' the whole magnetic configuration* (global problem!).

- *The Alfvén frequency vanishes for* $\mathbf{B} \cdot \nabla \sim k_{\parallel} = 0$.

  $\Rightarrow$ *Stability hinges on the smallness of the* $\mathbf{B} \cdot \nabla$ *operator,* so that the equilibrium should be known extremely accurately to produce the required balancing of large terms in numerical stability codes.

Statement of the equilibrium problem

- *To determine the magnetic confinement topology* (field lines, magnetic surfaces, curvatures, etc.) *of the 'most boring' case of plasma dynamics.*

  $\Rightarrow$ *Static equilibrium* ($\mathbf{v}_0 = 0$) $\equiv$ *absence of dynamics!*

Nonlinear MHD equations

- Conservation of **Mass:**

$$\frac{\partial \rho}{\partial t} = -\nabla \cdot (\rho \mathbf{v}) \,,$$

- Conservation of **Momentum:**

$$\rho \left(\frac{\partial}{\partial t} + \mathbf{v} \cdot \nabla \right) \mathbf{v} = -\nabla p + (\nabla \times \mathbf{B}) \times \mathbf{B} \,,$$

- Conservation of **Entropy:**

$$\left(\frac{\partial}{\partial t} + \mathbf{v} \cdot \nabla \right) p = -\gamma p \nabla \cdot \mathbf{v} \,,$$

- Conservation of **Magnetic Flux:**

$$\frac{\partial \mathbf{B}}{\partial t} = \nabla \times (\mathbf{v} \times \mathbf{B}) \,, \qquad \nabla \cdot \mathbf{B} = 0 \,.$$

$$\Rightarrow \quad \rho(\mathbf{r}, t) \,, \; \mathbf{v}(\mathbf{r}, t) \,, \; p(\mathbf{r}, t) \,, \; \mathbf{B}(\mathbf{r}, t) \,.$$

Static equilibrium equations

- MHD equations with $\partial/\partial t = 0$ an $\mathbf{v}_0 = 0$:

$$\mathbf{j} \times \mathbf{B} = \nabla p \qquad \textit{(pressure balance)}\,, \tag{1}$$

$$\mathbf{j} = \nabla \times \mathbf{B} \qquad \textit{(Ampère's law)}\,, \tag{2}$$

$$\nabla \cdot \mathbf{B} = 0 \qquad \textit{(THE law of magnetic fields)}\,. \tag{3}$$

- BC:

$$\mathbf{n} \cdot \mathbf{B} = 0 \qquad \textit{(at prescribed boundary)}\,. \tag{4}$$

$\Rightarrow$ **Nonlinear problem with an enormous amount of freedom:**

  – distribution of pressure and magnetic field,

  – shape of the boundary.

$\Rightarrow$ **Different alternatives for fusion experiments:**

  – pinches (1960) $\Rightarrow$ tokamaks/stellarators (1990) $\Rightarrow$ future devices (2020?).

Cylinder symmetry

- Rotation/translation symmetry: $\partial/\partial\theta = 0\,, \;\; \partial/\partial z = 0 \quad \Rightarrow \;\; B_r = 0\,, \;\; j_r = 0\,.$
- Profiles: $\rho(r)$ arbitrary, $p(r)$, $B_\theta(r)$, $B_z(r)$ *restricted by equilibrium:*

$$\left.\begin{aligned} \frac{dp}{dr} &= j_\theta B_z - j_z B_\theta \\ j_\theta = -\frac{dB_z}{dr} B_z\,, &\quad j_z = \frac{1}{r}\frac{d}{dr}(r B_\theta) \end{aligned}\right\} \;\Rightarrow\; \frac{d}{dr}(p + \tfrac{1}{2}B^2) = -\frac{B_\theta^2}{r}\,, \qquad (5)$$

  so that two of these profiles are arbitrary !

- For tokamaks, total pressure dominated by contribution of *magnetic pressure:*

$$\beta \equiv \frac{2p_0}{B_0^2} \ll 1 \quad \Rightarrow \quad P \equiv p + \tfrac{1}{2}B^2 \approx \tfrac{1}{2}B^2\,. \qquad (6)$$

  Numbers:

  $B = 3\,\mathrm{T} \quad \Rightarrow \quad P = 3.6 \times 10^6\,\mathrm{N/m^2} = 360$ metric tons $= 36\,\mathrm{atm}$ (on the coils)!

  $\beta = 0.03 \quad \Rightarrow \quad p \approx 1\,\mathrm{atm}$ (internally, and to be increased for future reactor)!

Cylindrical equilibria

Typical equilibrium profiles for:

θ–pinch

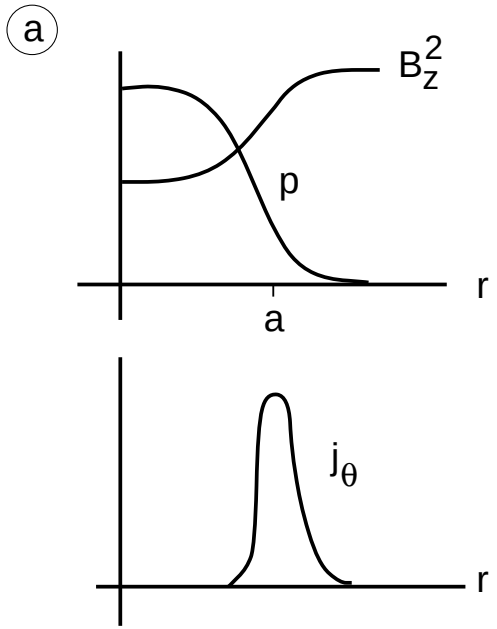

$$p + \tfrac{1}{2}B_z^2 = \text{const}$$

z-pinch

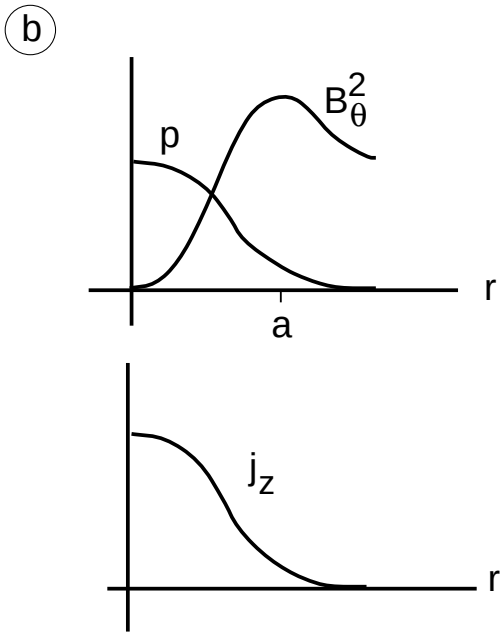

$$p + \tfrac{1}{2}B_\theta^2 = \text{const} - \int (B_\theta^2/r)\, dr$$

Rotational transform (periodic cylinder)

- Definition:

$$q_{\rm cyl} \equiv \frac{rB_z}{R_0 B_\theta} \quad \left(= \frac{2\pi r^2 B_z}{R_0 I_z} \right) . \tag{7}$$

- If **rational:**

$$q_{\rm cyl} = \frac{N}{M} \quad \left(= \frac{\text{number of toroidal revolutions}}{\text{number of poloidal revolutions}} \right) . \tag{8}$$

(a) (b)

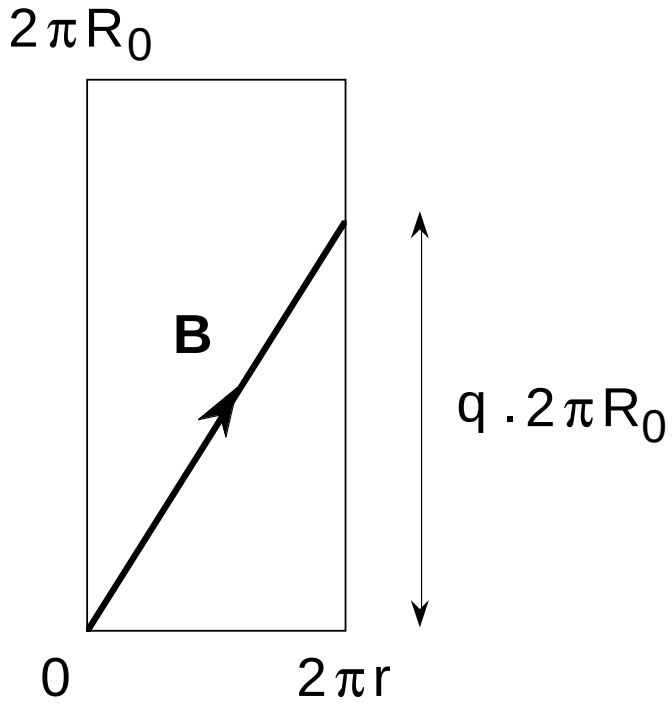

Cylindrical safety factor ($q < 1$)

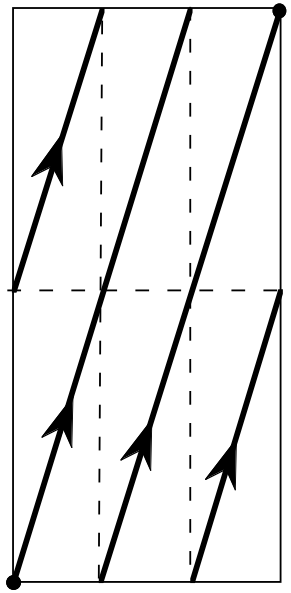

Rational field line ($q = 3/2$)

Rotational transform (cont'd)

- Perturbation on magnetic surface:

$$\sum_m \sum_n \xi_{r,mn}(r)\, \mathrm{e}^{\mathrm{i}(m\vartheta + n\varphi)} \,, \tag{9}$$

with poloidal angle $\vartheta \equiv \theta$, *toroidal angle* $\varphi \equiv z/R_0$, *toroidal mode number* $n \equiv kR_0$.

- **Parallel gradient operator:**

$$\mathbf{B} \cdot \nabla \xi_r \;\sim\; \mathbf{k} \cdot \mathbf{B}\, \xi_r \;\sim\; (m + nq)\, \xi_r \,. \tag{10}$$

$\Rightarrow$ **Rational field lines** with resonant perturbations crucial for instabilities:

$$q_{\mathrm{cyl}} = -\frac{m}{n} \qquad \left(= -\frac{\text{poloidal mode number}}{\text{toroidal mode number}} \right) \,. \tag{11}$$

- Orders of magnitude for periodic cylinder representing toroidal tokamak:

$$\epsilon \equiv a/R_0 \ll 1 \,, \quad B_\theta/B_0 \sim \epsilon \,, \quad B_z/B_0 \sim 1 \quad \Rightarrow \; q_{\mathrm{cyl}} \sim 1 \,. \tag{12}$$

- **Pressure effects,** represented by $\beta \equiv 2p_0/B_0^2 \sim \epsilon^2 \ll 1$, are not properly described by cylindrical approximation $\Rightarrow$ **require genuine toroidal theory!**

Toroidal equilibrium

Consequences of axisymmetry:

- Vector potential:

$$\nabla \cdot \mathbf{B} = 0 \quad \Rightarrow \quad \mathbf{B} = \nabla \times \mathbf{A}\,. \tag{13}$$

- **Poloidal magnetic flux** (renormalized with factor 2π) through area bounded by the *magnetic axis* (where $\Psi = 0$) and circle of radius R:

$$\Psi \equiv \frac{1}{2\pi}\iint \mathbf{B}\cdot\mathbf{n}\,dS = \frac{1}{2\pi}\oint \mathbf{A}\cdot d\boldsymbol{l} = -\int_0^{2\pi} A_\varphi d\varphi = -RA_\varphi\,. \tag{14}$$

$$\Rightarrow \quad B_R = \frac{\partial\,\mathrm{A}_\varphi}{\partial Z} = -\frac{1}{R}\frac{\partial\Psi}{\partial Z}\,, \quad B_Z = -\frac{1}{R}\frac{\partial}{\partial R}(RA_\varphi) = \frac{1}{R}\frac{\partial\Psi}{\partial R}\,, \tag{15}$$

- Ψ is a convenient label (kind of radial coordinate) for the *magnetic surfaces* spanned by $\mathbf{B}$ and $\mathbf{j}$, whereas ∇p is orthogonal to them.

- When the Poisson bracket of a function F and Ψ vanishes, then F is a *flux function:*

$$\{F,\Psi\} \equiv \mathbf{e}_\varphi\cdot(\nabla F\times\nabla\Psi) = \frac{\partial F}{\partial R}\frac{\partial\Psi}{\partial Z} - \frac{\partial F}{\partial Z}\frac{\partial\Psi}{\partial R} = 0 \quad \Rightarrow \; F = F(\Psi)\,. \tag{16}$$

Derivation Grad–Shafranov equation

(1) Divergence equation (3) and Ampere's law (2)

⇒ *poloidal field and current derivable from stream functions* $\Psi(R,Z)$ *and* $I(R,Z)$*:*

$$\nabla\cdot\mathbf{B}=\frac{1}{R}\frac{\partial(RB_R)}{\partial R}+\frac{\partial B_Z}{\partial Z}=0 \quad\Rightarrow\quad B_R=-\frac{1}{R}\frac{\partial\Psi}{\partial Z}\,,\quad B_Z=\frac{1}{R}\frac{\partial\Psi}{\partial R}\,, \tag{17}$$

$$\mathbf{j}=\nabla\times\mathbf{B}\quad\Rightarrow\quad\nabla\cdot\mathbf{j}=0\quad\Rightarrow\quad j_R=\frac{1}{R}\frac{\partial I}{\partial Z}\,,\qquad j_Z=-\frac{1}{R}\frac{\partial I}{\partial R}\,. \tag{18}$$

(2) Poloidal and toroidal components of Ampere's law (2)

⇒ *expressions for poloidal current stream function* I *and toroidal current* j_φ*:*

$$j_R=\frac{\partial B_\varphi}{\partial Z}\,,\quad j_Z=-\frac{1}{R}\frac{\partial(RB_\varphi)}{\partial R}\qquad\Rightarrow\quad I\equiv RB_\varphi\,, \tag{19}$$

$$Rj_\varphi=R\left(\frac{\partial B_z}{\partial R}-\frac{\partial B_R}{\partial Z}\right)=R\frac{\partial}{\partial R}\left(\frac{1}{R}\frac{\partial\Psi}{\partial R}\right)+\frac{\partial^2\Psi}{\partial Z^2}\equiv\Delta^*\Psi \text{ (quasi-Lapl.)}. \tag{20}$$

(3) Toroidal and poloidal components of pressure balance equation (1)

$\Rightarrow$ I **and** p **are flux functions** (functions of Ψ) and related to j_φ:

$$\frac{\partial p}{\partial \varphi} = j_R B_Z - j_Z B_R = \frac{1}{R^2}\left(\frac{\partial I}{\partial Z}\frac{\partial \Psi}{\partial R} - \frac{\partial I}{\partial R}\frac{\partial \Psi}{\partial Z}\right) = 0 \quad \Rightarrow \quad I \equiv I(\Psi)\,, \tag{21}$$

$$\left.\begin{aligned} \frac{\partial p}{\partial R} &= j_Z B_\varphi - j_\varphi B_Z = \left(-\frac{I I'}{R^2} - \frac{j_\varphi}{R}\right)\frac{\partial \Psi}{\partial R} \\ \frac{\partial p}{\partial Z} &= j_\varphi B_R - j_R B_\varphi = \left(-\frac{I I'}{R^2} - \frac{j_\varphi}{R}\right)\frac{\partial \Psi}{\partial Z} \end{aligned}\right\} \Rightarrow \left\{\begin{aligned} & p = p(\Psi)\,, \\ & -\frac{I I'}{R^2} - \frac{j_\varphi}{R} = p'\,. \end{aligned}\right. \tag{22}$$

(4) From Eqs. (37) and (22)

$\Rightarrow$ **equilibrium described by Grad–Shafranov equation:**

$$[\,\Delta^*\Psi \equiv\,] \quad R\frac{\partial}{\partial R}\left(\frac{1}{R}\frac{\partial \Psi}{\partial R}\right) + \frac{\partial^2 \Psi}{\partial Z^2} = -I I' - R^2 p' \quad [\,= R j_\varphi\,]\,, \tag{23}$$

elliptic nonlinear PDE that has to satisfy the BC

$$\Psi = \text{const} \quad \text{(on the plasma cross-section)}\,. \tag{24}$$

Geometry

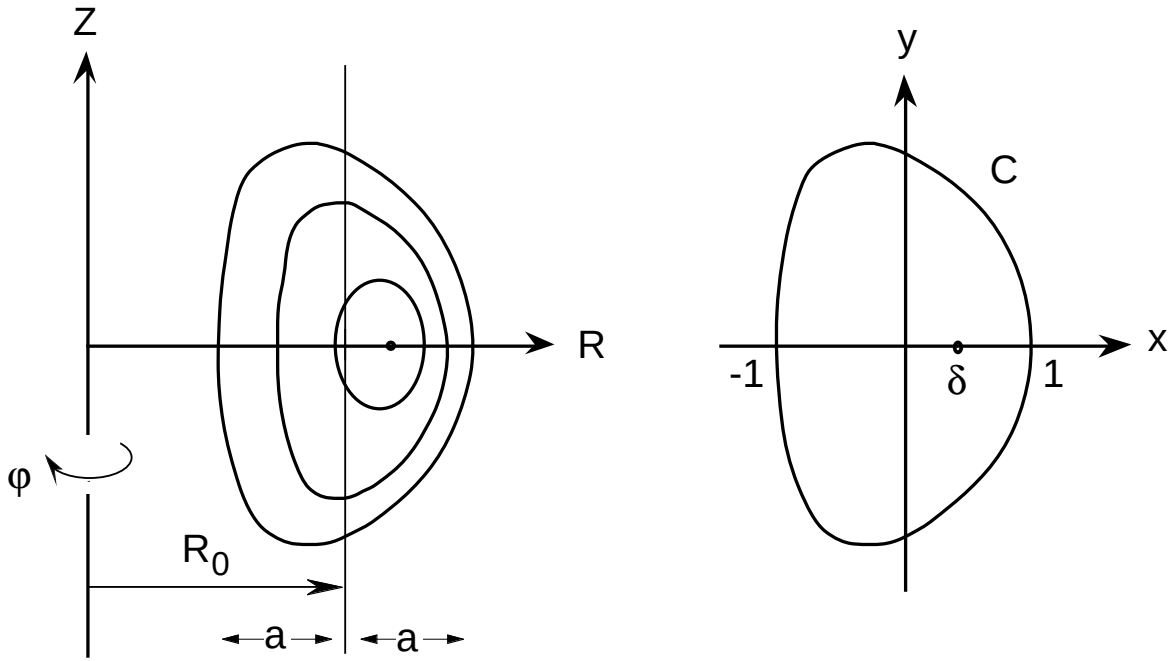

Cross-sectional shape poloidal x-y plane.

- Cartesian coordinates: $x \equiv (R - R_0)/a\,, \qquad y \equiv Z/a\,,$ (25)
- Inverse aspect ratio: $\epsilon \equiv a/R_0 \quad (\ll 1$ in asymptotic expansions $)\,.$ (26)

Scaling

(1) *Unit flux label* (Ψ_1 is total poloidal flux through plasma):

$$\psi \equiv \Psi/\Psi_1 \quad \Rightarrow \quad 0 \le \psi \le 1\,, \tag{27}$$

and *dimensionless inverse flux*:

$$\alpha \equiv a^2 B_0/\Psi_1 \qquad (\text{related to edge safety factor: } q_1 \sim \alpha)\,. \tag{28}$$

(2) Dimensionless *unit profiles and amplitudes* A and B:

$$\frac{\alpha}{B_0}\big[II' + \frac{a^2}{\epsilon^2}p'\big] \;\equiv\; -A\Gamma(\psi)\,, \qquad \Gamma(0)=1\,, \quad \Gamma(1)=0\,, \tag{29}$$

$$\frac{\alpha a^2}{\epsilon B_0}p' \;\equiv\; -\tfrac{1}{2}AB\Pi(\psi)\,, \qquad \Pi(0)=1\,, \quad \Pi(1)=0\,.$$

(3) The Grad–Shafranov equation then becomes:

$$\psi_{xx} + \psi_{yy} - \epsilon(1+\epsilon x)^{-1}\,\psi_x = A[\,\Gamma(\psi) + Bx(1+\tfrac{1}{2}\epsilon x)\Pi(\psi)\,]\,, \tag{30}$$

with BCs:

$$\psi = 1 \qquad \text{at plasma boundary } C \;\; (r = f(\theta)), \tag{31}$$

$$\psi = \psi_x = \psi_y = 0 \quad \text{at magnetic axis} \quad (x=\delta,\; y=0). \tag{32}$$

$\Rightarrow$ For given δ, constants A and B eigenvalues to be determined together with ψ.

Equilibrium solver: parameters

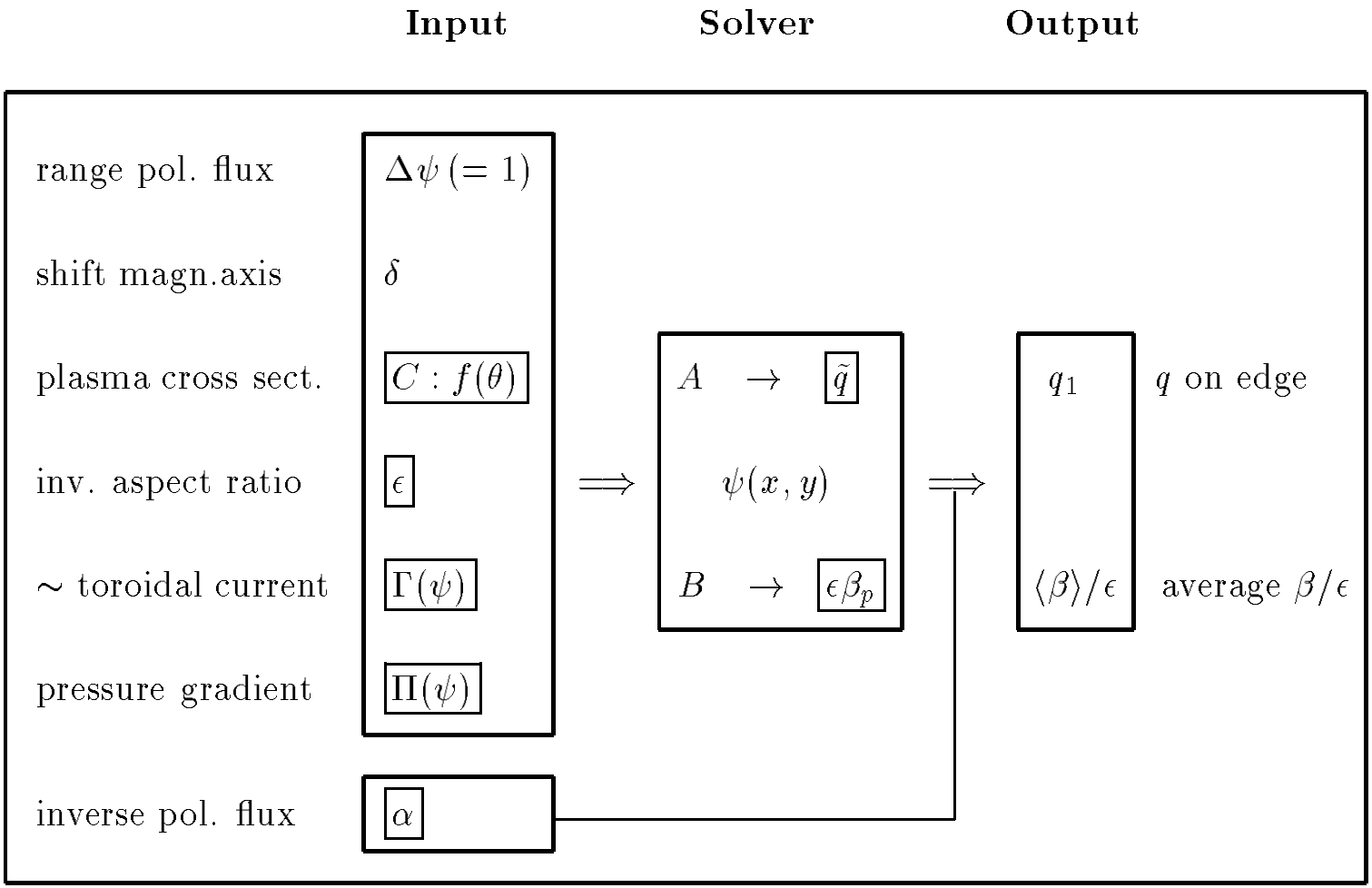

Independent (boxed) parameters and profiles in numerical equilibrium solver.

Straight field line coordinates

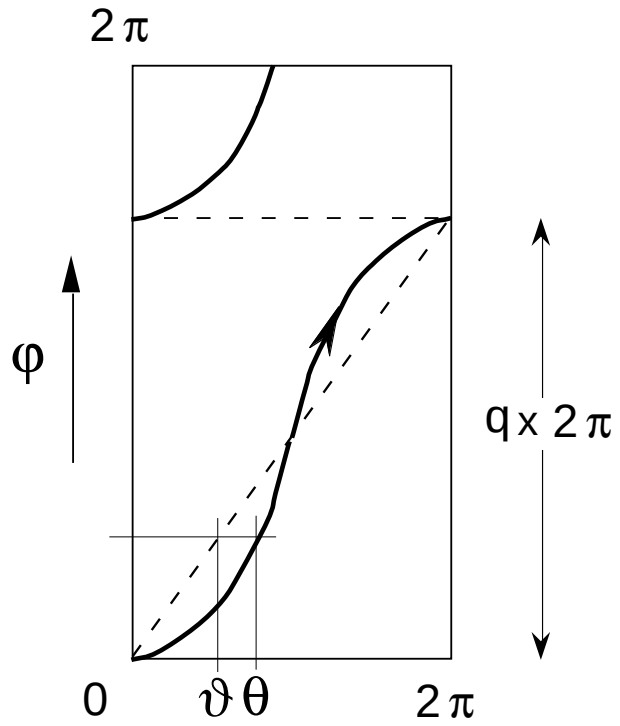

Construction of the angle ϑ from θ

- These permit simple representation of parallal gradient operator. They require a coordinate inversion:

$$\begin{array}{l}\psi = \psi(x_i, y_j) \\ \vartheta = \vartheta(x_i, y_j)\end{array} \quad \Rightarrow \quad \begin{array}{l}x = x(\psi_i, \vartheta_j) \\ y = y(\psi_i, \vartheta_j)\end{array} \quad .$$

- All quantities in the stability analysis are transformed to ψ, ϑ, φ coordinates, i.e. normal field line curvature κ_n, geodesic curvature κ_g, toroidal current j_φ, etc. These involve second derivatives with respect to ψ so that equilibrium solutions need to be surprisingly accurate for a reliable stability analysis.

Uncertainty

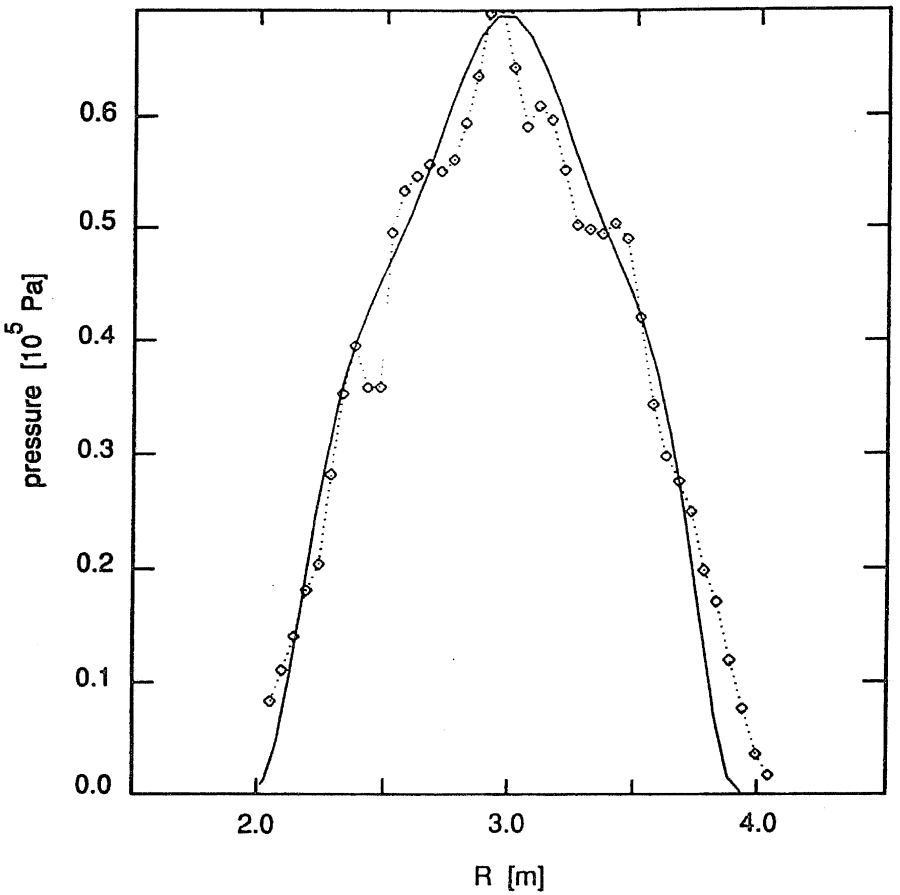

Smoothing experimental data to obtain equilibrium profiles for stability studies:

- inaccurate experimental data

  or

- neglecting essential 3D deviations (magnetic islands) from axisymm.?

Electron pressure profile obtained by LIDAR diagnostic at JET (dashed with diamonds) and reconstructed pressure profile by means of an equilibrium solver (drawn). [Huysmans *et al.*, Phys. Fluids **B5**, 1545 (1993)].

Toroidal wave equation

- Linearise MHD equations:

$$f(\mathbf{r},t) \approx f_0(\psi,\vartheta) + f_1(\psi,\vartheta)\mathrm{e}^{\mathrm{i}(n\varphi-\omega t)}, \tag{33}$$

where n is the toroidal mode number.

- Exploit *projection based on magnetic surfaces and field lines*, involving field line triad

$$\mathbf{n} \equiv \nabla\psi/|\nabla\psi|\,, \quad \boldsymbol{\pi} \equiv \mathbf{b}\times\mathbf{n}\,, \quad \mathbf{b} \equiv \mathbf{B}/B\,. \tag{34}$$

$\Rightarrow$ Gradient operator:

$$\begin{aligned} D &\equiv (RB_p)^{-1}\mathbf{n}\cdot\nabla &&= \partial_\psi - (g_{12}/g_{22})\,\partial_\vartheta\,, \\ G &\equiv -\mathrm{i}\mathbf{B}\times\nabla\psi\cdot\nabla &&= -\mathrm{i}IJ^{-1}\partial_\vartheta - nB_p^2\,, \\ F &\equiv -\mathrm{i}\mathbf{B}\cdot\nabla &&= J^{-1}(-\mathrm{i}\partial_\vartheta + nq)\,. \end{aligned} \tag{35}$$

$\Rightarrow$ Displacement vector:

$$X \equiv RB_p\,\boldsymbol{\xi}\cdot\mathbf{n}\,, \quad Y \equiv \frac{\mathrm{i}}{RB_p}\,\boldsymbol{\xi}\cdot\boldsymbol{\pi}\,, \quad Z \equiv \frac{\mathrm{i}}{B}\,\boldsymbol{\xi}\cdot\mathbf{b}\,. \tag{36}$$

- This gives the *toroidal wave equation* (Goedbloed, Phys. Fluids **18**, 1258 (1975)):

$$\begin{pmatrix} \mathcal{A}_{11} & \mathcal{A}_{12} & \mathcal{A}_{13} \\ \mathcal{A}_{21} & \mathcal{A}_{22} & \mathcal{A}_{23} \\ \mathcal{A}_{31} & \mathcal{A}_{32} & \mathcal{A}_{33} \end{pmatrix} \begin{pmatrix} X \\ Y \\ Z \end{pmatrix} = -\rho\omega^2 \begin{pmatrix} \mathcal{B}_{11}\, X \\ \mathcal{B}_{22}\, Y \\ \mathcal{B}_{33}\, Z \end{pmatrix}, \qquad (37)$$

where

$$\mathcal{A}_{11} \equiv D(\gamma p + B^2)D^\dagger - F\frac{1}{R^2B_p^2}F - E\,, \qquad \mathcal{A}_{31} \equiv -F\gamma p D^\dagger\,,$$

$$\mathcal{A}_{12} \equiv DG\frac{\gamma p + B^2}{B} - 2(\frac{B_\varphi \kappa_t}{B_p}\frac{\mathrm{i}}{J}\partial_\vartheta + \frac{B_p\kappa_p}{R}n)B\,, \qquad \mathcal{A}_{32} \equiv -F\gamma p G\frac{1}{B}\,,$$

$$\mathcal{A}_{13} \equiv D\gamma p F\,, \qquad \mathcal{A}_{33} \equiv -F\gamma p F\,,$$

$$\mathcal{A}_{21} \equiv -\frac{\gamma p + B^2}{B}GD^\dagger - 2B(\frac{\mathrm{i}}{J}\partial_\vartheta\frac{B_\varphi\kappa_t}{B_p} + n\frac{B_p\kappa_p}{R})\,, \qquad \mathcal{B}_{11} \equiv \frac{1}{R^2B_p^2}\,,$$

$$\mathcal{A}_{22} \equiv -\frac{1}{B}G\gamma p G\frac{1}{B} - BG\frac{1}{B^2}GB - BF\frac{R^2B_p^2}{B^2}FB\,, \qquad \mathcal{B}_{22} \equiv R^2B_p^2\,,$$

$$\mathcal{A}_{23} \equiv -\frac{1}{B}G\gamma p F\,, \qquad \mathcal{B}_{33} \equiv B^2\,.$$

Further directions

- **Continuous spectra** (local to magnetic surfaces):

  $\Rightarrow$ *take limit* $D \rightarrow \infty$*.*

- **Ballooning modes** (local to field lines):

  $\Rightarrow$ *more subtle limit to isolate pressure driven instabilities.*

- **Mercier criterion** (local to magnetic surfaces):

  $\Rightarrow$ *contained in ballooning procedure, also pressure driven modes.*

- **Numerical work** (global waves and instabilities):

  $\Rightarrow$ *exploiting quadratic forms (Galerkin method).*

Alfvén and slow continuum modes

- *Magnetic surface resonances* (limit $D \to \infty$):

$$D^\dagger X \approx -\frac{1}{\gamma p + B^2}[\, G\frac{\gamma p + B^2}{B} Y + \gamma p F Z \,]\,. \tag{38}$$

Substituting into second and third component of Eq. (17) leads to a system of two differential equations for Y and Z where the normal derivative no longer appears.

- $\Rightarrow$ Modes localised about single magnetic surface:

$$\boldsymbol{\xi}(\psi,\vartheta,\varphi) \approx -\mathrm{i}\delta(\psi-\psi_0)\,[\,\eta(\vartheta)\boldsymbol{\pi} + \zeta(\vartheta)\mathbf{b}\,]\,\mathrm{e}^{\mathrm{i}n\varphi}, \tag{39}$$

with the two tangential components

$$\eta \equiv \boldsymbol{\xi}\cdot\boldsymbol{\pi} \equiv -\mathrm{i}RB_p Y\,, \qquad \zeta \equiv \boldsymbol{\xi}\cdot\mathbf{b} \equiv -\mathrm{i}BZ\,,$$

which satisfy a system of two ODEs (repeated on next page):

$$\begin{pmatrix} \alpha_{11} & \alpha_{12} \\ \alpha_{21} & \alpha_{22} \end{pmatrix} \begin{pmatrix} \eta \\ \zeta \end{pmatrix} = \rho\omega^2 \begin{pmatrix} \eta \\ \zeta \end{pmatrix}.$$

Alfvén and slow continuum modes (cont'd)

- Tangential components satisfy a system of two ODEs (Goedbloed, 1975):

$$\begin{pmatrix} \alpha_{11} & \alpha_{12} \\ \alpha_{21} & \alpha_{22} \end{pmatrix} \begin{pmatrix} \eta \\ \zeta \end{pmatrix} = \rho\omega^2 \begin{pmatrix} \eta \\ \zeta \end{pmatrix}, \tag{40}$$

  where

$$\alpha_{11} \equiv \frac{B}{RB_p} F \frac{R^2 B_p^2}{B^2} F \frac{B}{RB_p} + \frac{4\gamma p B^2}{\gamma p + B^2} \kappa_g^2 , \qquad \alpha_{21} \equiv \mathrm{i} \frac{1}{B} F \frac{2\gamma p B^2}{\gamma p + B^2} \kappa_g ,$$

$$\alpha_{12} \equiv -\mathrm{i} \frac{2\gamma p B^2}{\gamma p + B^2} \kappa_g F \frac{1}{B} , \qquad \alpha_{22} \equiv \frac{1}{B} F \frac{\gamma p B^2}{\gamma p + B^2} F \frac{1}{B} .$$

- Two coupled ODEs $\Rightarrow$ **Toroidal Alfvén and slow continuum modes**.
- Cylindrical limit ($\epsilon \longrightarrow 0$) :

$$\omega_A = (m + nq)\, B_\theta / (r\sqrt{\rho}) , \quad \eta_A \sim \delta(r - r_A) ,$$

$$\omega_S = \sqrt{\gamma p / (\gamma p + B^2)}\, \omega_A , \quad \zeta_S \sim \delta(r - r_S) . \tag{41}$$

Continuous spectrum

Numerical solution (Poedts et al, PPCF **34**, 1397 (1992)), continua with gaps:

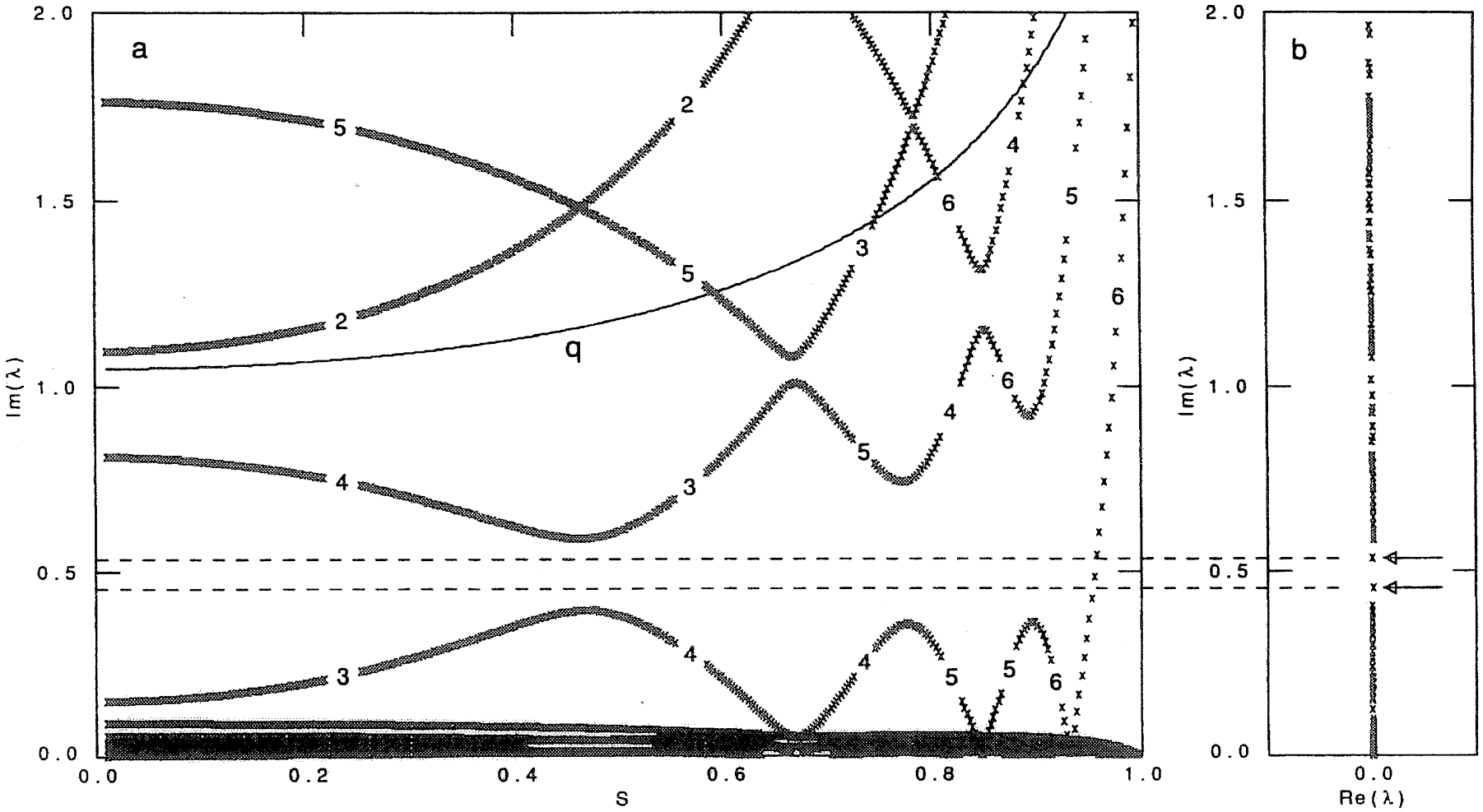

In those gaps: **Toroidal Alfvén Eigenmodes (TAEs).**

Alfvén and slow ballooning modes

- *Magnetic field line resonances*: Reconcile field line localisation with poloidal and toroidal periodicity by *ballooning transformation* to extended poloidal angle $-\infty < \vartheta < \infty$ (Connor, Hastie, Taylor, Proc. Roy. Soc. **A365**, 1 (1999)).

  Ballooning modes are WKB solutions on extended domain:

$$\boldsymbol{\xi}(\psi,\vartheta,\varphi) = \widetilde{\boldsymbol{\xi}}(\psi,\vartheta)\,\mathrm{e}^{\mathrm{i}nS(\psi,\vartheta,\varphi)}\,, \tag{42}$$

  where $n \gg 1$. Eikonal:

$$S = \varphi - q(\vartheta - \vartheta_0)\,. \tag{43}$$

- Renormalise local wave number $\mathbf{k}_\perp = n\nabla S$:

$$\begin{aligned} \bar{\mathbf{k}} \equiv \mathbf{k}_\perp/n = \nabla S &= \bar{k}_n\mathbf{n} + \bar{k}_\pi\boldsymbol{\pi}\,, \\ \bar{k}_n &= -RB_p\left[q'(\vartheta-\vartheta_0) - (g_{12}/g_{22})q\right], \\ \bar{k}_\pi &= -B/(RB_p)\,, \end{aligned} \tag{44}$$

- Project on new orthogonal triad $\mathbf{e} \equiv \mathbf{k}_\perp/k_\perp\,, \mathbf{d}\,, \mathbf{b}$:
  $\Rightarrow$ new components $\tilde{u}, \tilde{v}, \tilde{\zeta}$ of vector $\boldsymbol{\xi}$.

Alfvén and slow ballooning modes (cont'd)

- Ballooning modes are perpendicular to $\mathbf{k}_\perp$, $\tilde{u} \equiv i\mathbf{e}\cdot\boldsymbol{\xi} \approx 0$, i.e. are described by two components,

$$\widetilde{\boldsymbol{\xi}}(\psi,\vartheta) \approx -\mathrm{i}\left[\,\tilde{v}(\psi,\vartheta)\mathbf{d} + \tilde{\zeta}(\psi,\vartheta)\mathbf{b}\,\right], \tag{45}$$

- which satisfy a *system of two ODEs* (Dewar & Glasser, Phys. Fluids **26**, 3038 (1983)):

$$\begin{pmatrix} \tilde{\alpha}_{11} & \tilde{\alpha}_{12} \\ \tilde{\alpha}_{21} & \tilde{\alpha}_{22} \end{pmatrix} \begin{pmatrix} \tilde{v} \\ \tilde{\zeta} \end{pmatrix} = \rho\omega^2 \begin{pmatrix} \tilde{v} \\ \tilde{\zeta} \end{pmatrix}, \tag{46}$$

$$\tilde{\alpha}_{11} \equiv \frac{B}{\bar{k}}\tilde{F}\frac{\bar{k}^2}{B^2}\tilde{F}\frac{B}{\bar{k}} + \frac{4\gamma p B^2}{\gamma p + B^2}\kappa_d^2 - 2\frac{B}{\bar{k}}\kappa_d p' \,, \qquad \tilde{\alpha}_{21} \equiv \mathrm{i}\frac{1}{B}\tilde{F}\frac{2\gamma p B^2}{\gamma p + B^2}\kappa_d \,,$$

$$\tilde{\alpha}_{21} \equiv \mathrm{i}\frac{1}{B}\tilde{F}\frac{2\gamma p B^2}{\gamma p + B^2}\kappa_d \,, \qquad \tilde{\alpha}_{22} \equiv \frac{1}{B}\tilde{F}\frac{\gamma p B^2}{\gamma p + B^2}\tilde{F}\frac{1}{B} \,. \tag{47}$$

- Two coupled ODEs $\Rightarrow$ **Toroidal Alfvén and slow ballooning modes**.
- Ballooning mode analysis in tokamaks: *instabilities at high beta driven by the pressure gradient p' and the curvature of the field lines*.

Two directions in local analysis

- *Stability of tokamaks*: ballooning term $\kappa_d\, p' \approx \kappa_t\, p'$ dominates
  (instability searches out the worst conditions for confinement).
- *Alfvén wave heating*: ballooning term $\kappa_d\, p'$ unimportant
  (excitation forces stable waves of a fixed frequency onto the system).

Mercier criterion

- Derived by Mercier, Nucl. Fusion **1**, 47 (1960), generalisation of Suydam criterion.
  (New interpretion: condition for clustering of ballooning solutions for $\vartheta \to \infty$.)
- The following expression is obtained:

$$\left[\pi q' - I p' \oint \frac{1}{R^2 B_p^2} J d\vartheta\right]^2 + p' \oint \frac{B^2}{R^2 B_p^2} J d\vartheta \times \left[2 \oint \frac{\kappa_p}{R B_p} J d\vartheta + I I' \oint \frac{1}{R^2 B_p^2} J d\vartheta\right] > 0\,. \qquad (48)$$

Global analysis (necessarily numerical):

Ideal MHD

- Ideal MHD codes: ERATO, PEST, . . .

Resistive MHD

- Resistive MHD codes: NOVA, CASTOR, MARS, . . .
- Results CASTOR

Troyon limit

- Theoretical limit for *kink & ballooning stability* :

$$\beta\,(\%) < g_{\mathrm{T}} \frac{I\,(\mathrm{MA})}{a\,(\mathrm{m})\,B\,(\mathrm{T})}\,,$$

- But experimental points cross the curve!
- Present experimental limit (DIIID) :

$$\beta \sim 10\%\,.$$

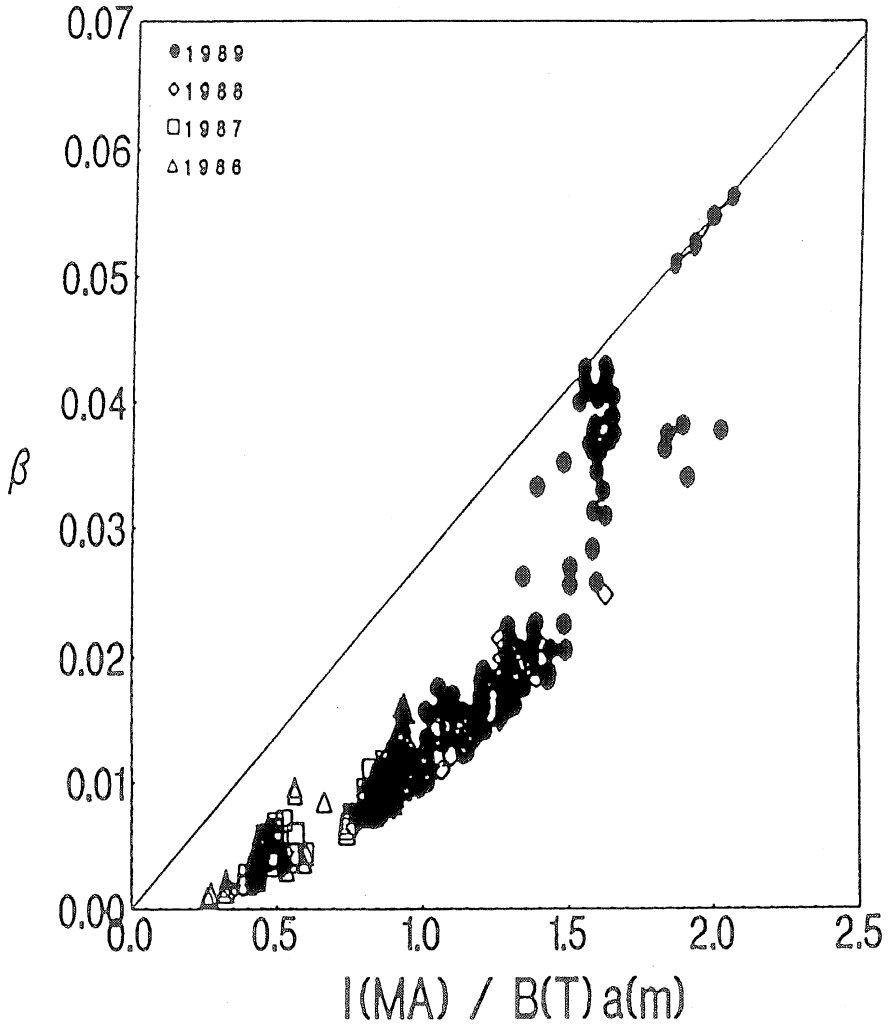

Linearised Resistive MHD equations

- Dissipative MHD : variable $\boldsymbol{\xi}$ no longer available since it is based on flux conservation.
  $\Rightarrow$ Return to primitive variables of resistive MHD.
- Eigenvalue problem :

$$\lambda\rho_1 = -\nabla\cdot(\rho\mathbf{v}_1)\,, \tag{49}$$

$$\lambda\rho\mathbf{v}_1 = -\nabla(\rho\,T_1+(p/\rho)\,\rho_1)+(\nabla\times\mathbf{B})\times(\nabla\times\mathbf{A}_1) -\mathbf{B}\times(\nabla\times\nabla\times\mathbf{A}_1)\,, \tag{50}$$

$$\lambda\rho T_1 = -\rho\mathbf{v}_1\cdot\nabla(p/\rho)-p\nabla\cdot\mathbf{v}_1 +2\eta\,(\gamma-1)\,(\nabla\times\mathbf{B})\cdot(\nabla\times\nabla\times\mathbf{A}_1)\,, \tag{51}$$

$$\lambda\mathbf{A}_1 = -\mathbf{B}\times\mathbf{v}_1-\eta\,\nabla\times\nabla\times\mathbf{A}_1\,. \tag{52}$$

- Basic state represented by 8-vector :

$$\mathbf{U}\equiv[\,\rho_1,\mathbf{v}_1,T_1,\mathbf{A}_1\,]^{\mathrm{T}}\,, \tag{53}$$

Two Approaches:

Conservative

- **Ideal MHD** with $\mathbf{v}_1 \equiv \partial\boldsymbol{\xi}/\partial t$:

$$\mathbf{F}(\boldsymbol{\xi}) = \rho\frac{\partial^2\boldsymbol{\xi}}{\partial t^2} = -\rho\omega^2\boldsymbol{\xi}\,, \tag{54}$$

  where $\mathbf{F}$ is self-adjoint and eigenvalues ω^2 are real.

Dissipative

- **Resistive MHD** with $\mathbf{U} \equiv [\rho_1, \mathbf{v}_1, T_1, \mathbf{B}_1]^T$:

$$\mathbf{L}\cdot\mathbf{U} = \mathbf{R}\cdot\frac{\partial\mathbf{U}}{\partial t} = \lambda\,\mathbf{R}\cdot\mathbf{U}\,, \tag{55}$$

  where $\mathbf{L}$ is non-Hermitian and $\lambda \equiv -i\omega$ is complex.

CASTOR & POLLUX (tokamak) (coronal loop)

- Resistive eigenvalue problem $\mathbf{L} \cdot \mathbf{U} = \lambda \, \mathbf{R} \cdot \mathbf{U}$ solved by Galerkin method:

$$\int \mathbf{V}^{\mathrm{T}} \cdot \mathbf{L} \cdot \mathbf{U} \, dV = \lambda \int \mathbf{V}^{\mathrm{T}} \cdot \mathbf{R} \cdot \mathbf{U} \, dV \, . \tag{56}$$

- FEM (r) and FFT (ϑ) discretisation of $\mathbf{U}$ and $\mathbf{V}$:

$$\mathbf{A} \cdot \mathbf{x} = -\lambda \, \mathbf{B} \cdot \mathbf{x} \, , \tag{57}$$

  where $\mathbf{A}$ and $\mathbf{B}$ are large non-Hermitian matrices.

- Forced oscillations (excitation):

$$(\mathbf{A} + i\omega_d \mathbf{B}) \cdot \mathbf{x} = \mathbf{f} \, , \tag{58}$$

  with driving frequency ω_d and forcing term $\mathbf{f}$.

CASTOR dicretization

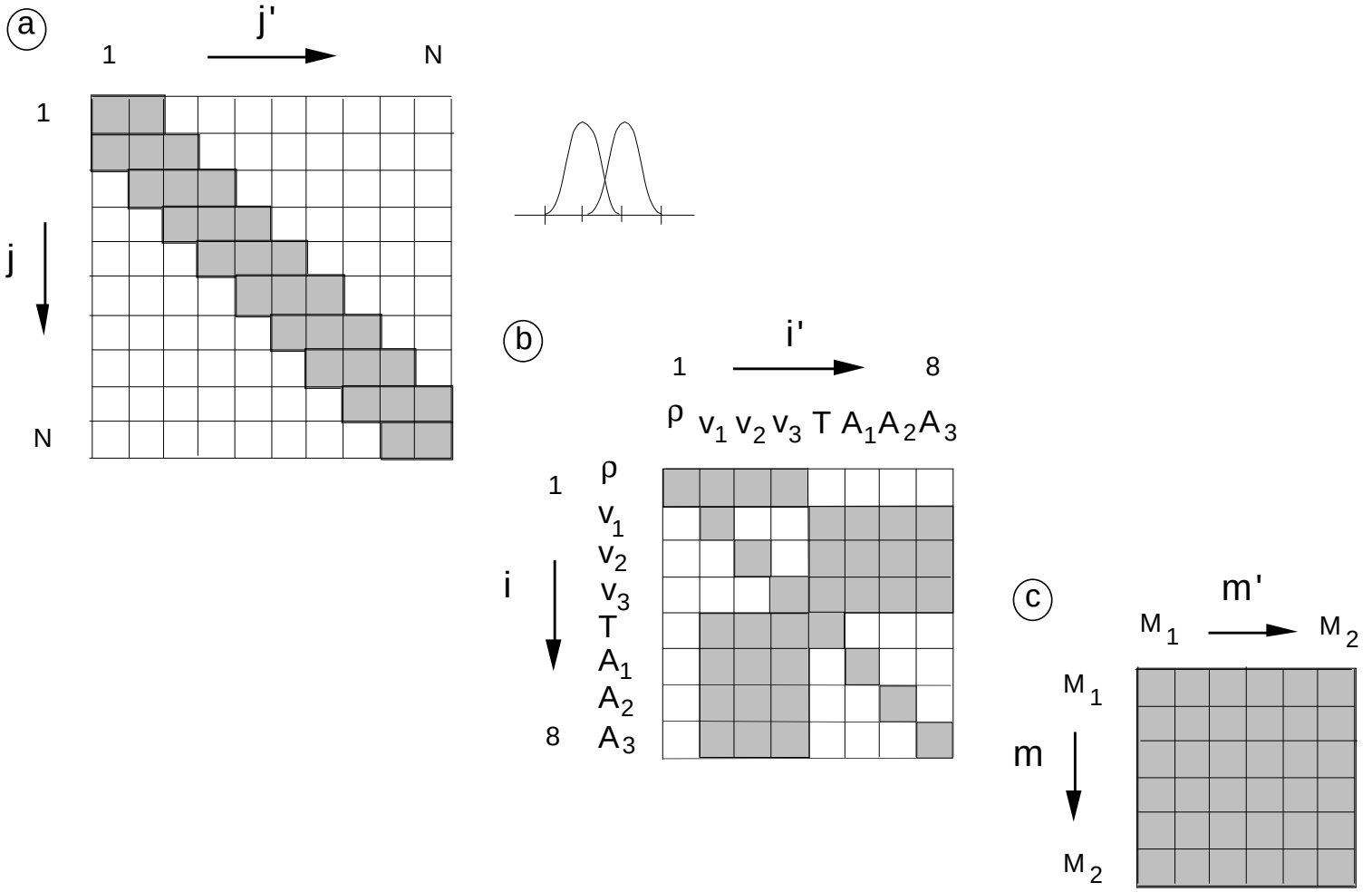

Typical MHD stability study

- **ELMs in JET :**

  Playing with the equilibrium profiles, edge current density j_φ (JET # 23336)

  $\Rightarrow$ $n = 1$ free-boundary tearing modes,

  $\Rightarrow$ $n = 4$ pressure-driven modes.

- General philosophy :

  Comparing experimental data on instabilities with theoretical results

  $\Rightarrow$ **MHD Spectroscopy.**

Free-boundary tearing mode

- Flux averaged toroidal current profiles and corresponding growth rates as a function of the resistivity for the $n = 1$ free boundary tearing mode.

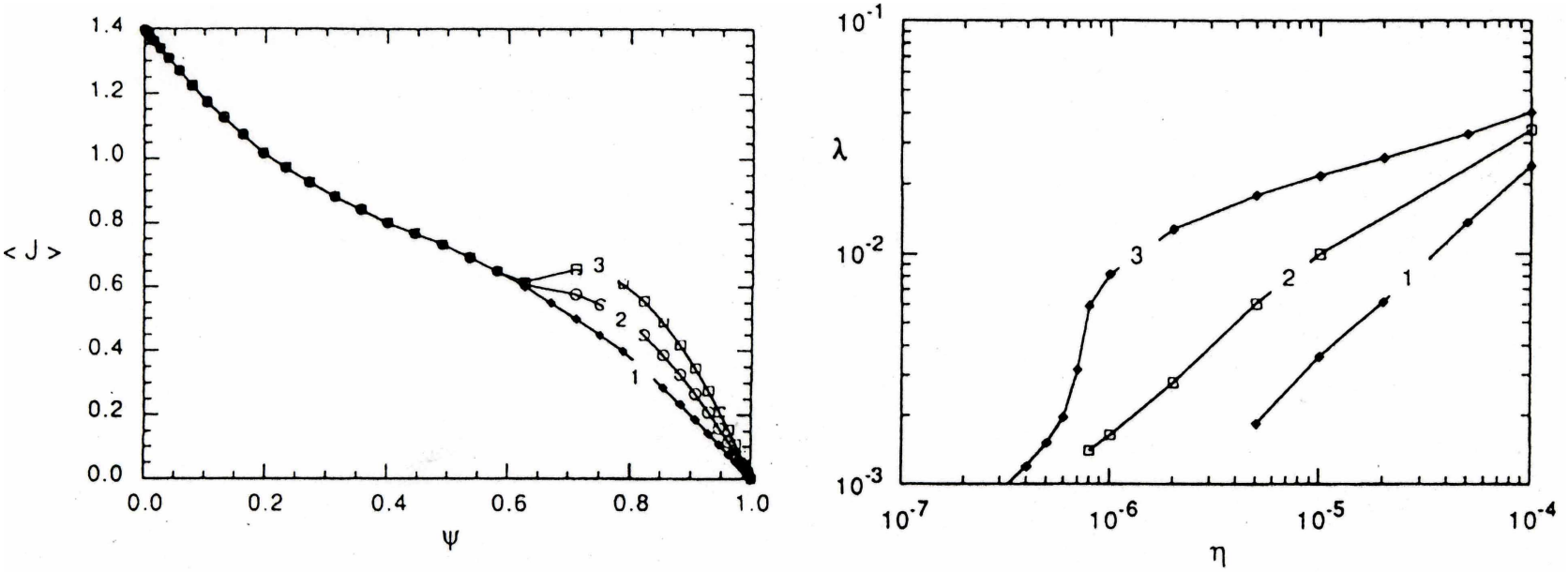

- Reconstructed profile (labelled by 1) produces growth rate that is insignificant for the relevant values of the edge resistivity. Artificial increase of the shoulder on the current density profile (curve labelled by 3) produces large growth rates with threshold that could facilitate ELMs by sudden increase of resistivity due to edge cooling.

External resistive mode

- Poloidal velocities of an $n = 4$ external resistive mode (JET discharge # 27793).

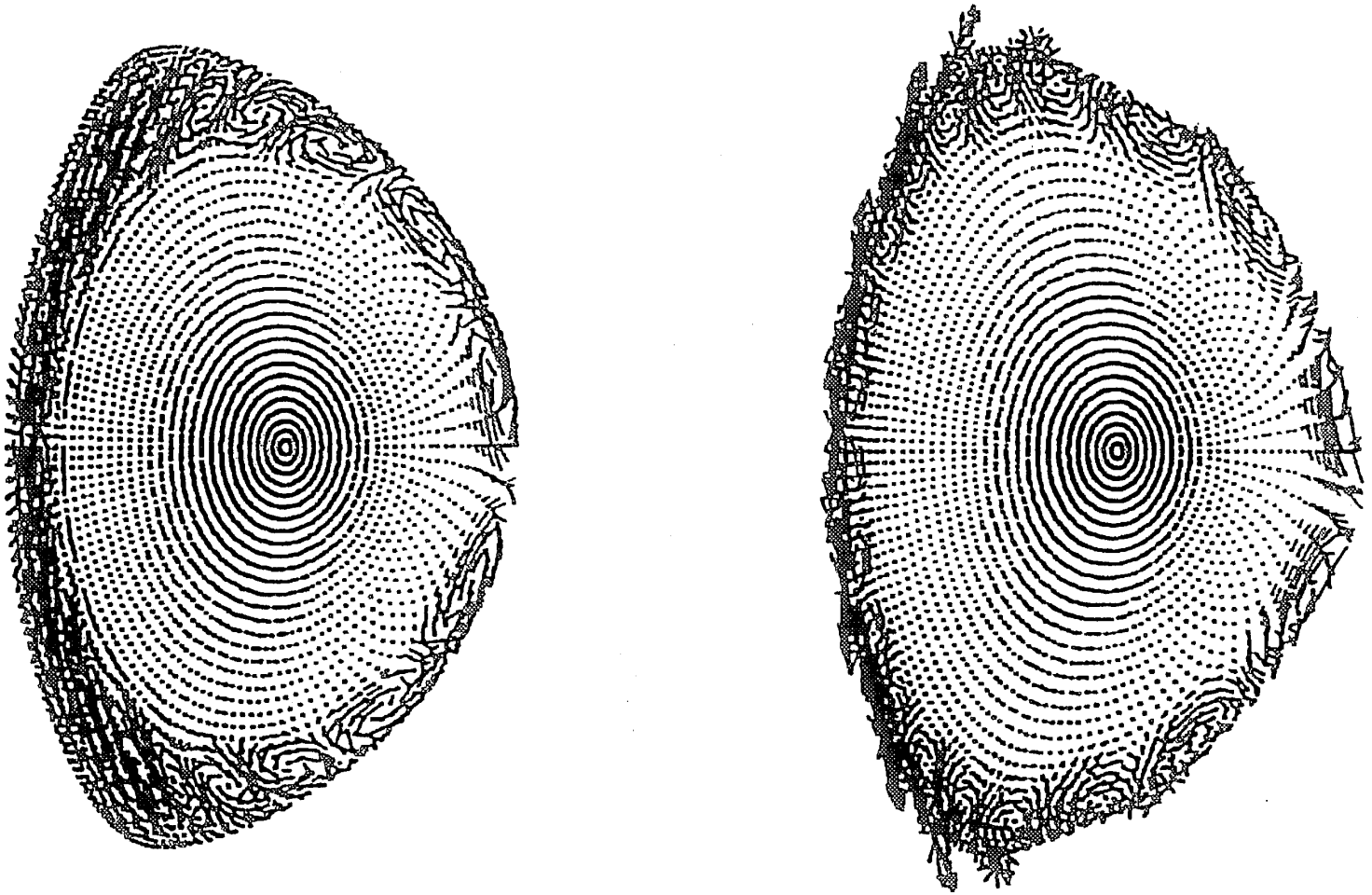

- Internal $n = 4$ mode at $q = 3$ (left), for larger current mode becomes external (right).

MHD spectroscopy

- Computed response to $n = 1$ field perturbation induced by saddle coils at JET: TAE (toroidicity $\Delta m = 1$), EAE (ellipticity $\Delta m = 2$) and BAE (β induced):

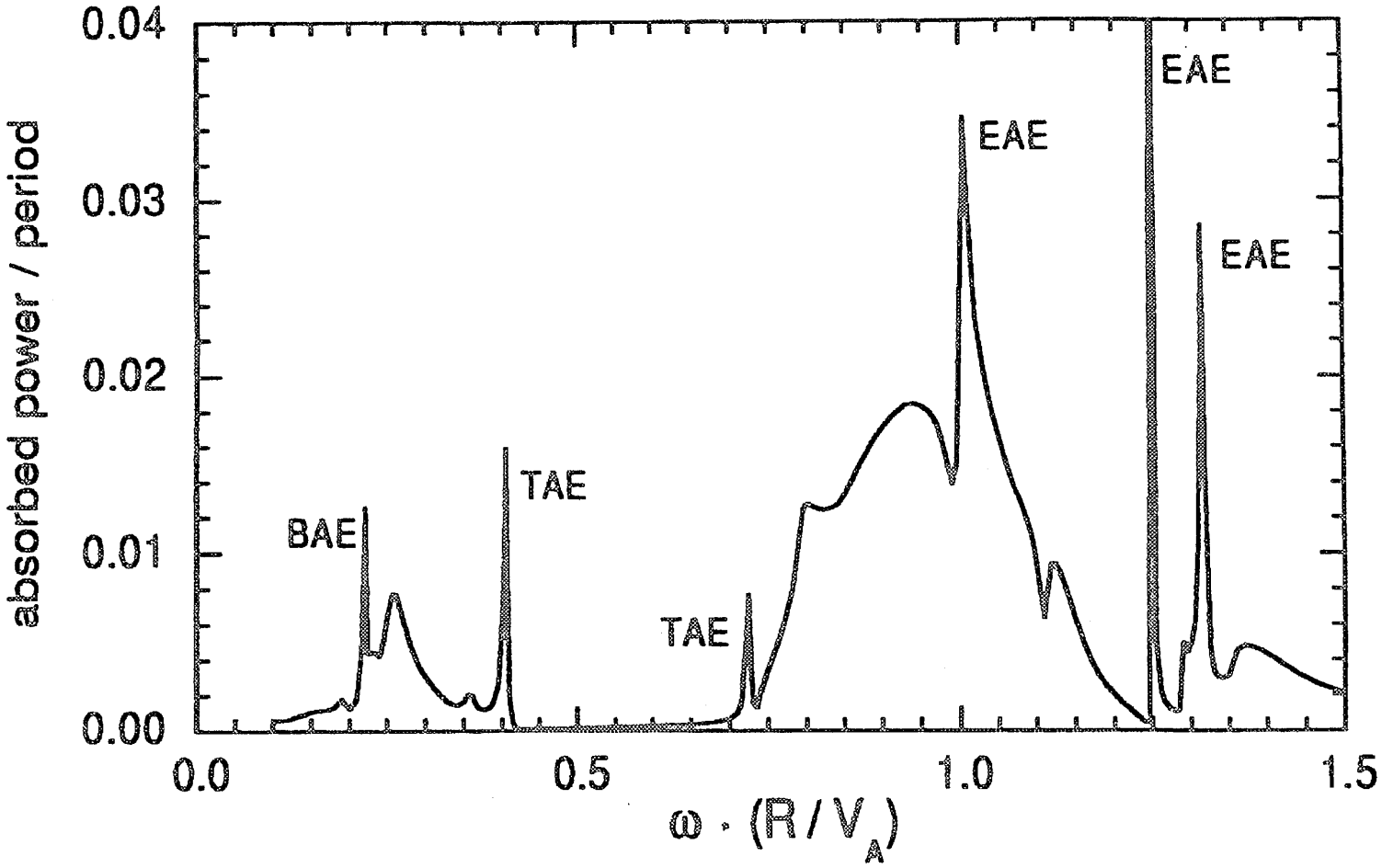

MHD spectroscopy (cont'd)

Music of the tokamak! (SOUND.WAV)

MHD wave signals picked up by an external coil, with artificial decrease (10^{-3}) of the frequency

(sound track Igor Semenov, Moscow)